19 Towards Quantum Logic with Cold Atoms in a CO_2-Laser Optical Lattice

G. Cennini, G. Ritt, C. Geckeler, R. Scheunemann, and M. Weitz

Physikalisches Institut der Universität Tübingen
Auf der Morgenstelle 14
72076 Tübingen
Germany

19.1 Introduction

Recent progress in the field of quantum optics has opened the door to an increasing number of fascinating applications ranging from the generation of entangled quantum states [1] to the production and manipulation of Bose-Einstein condensates of atomic gases [2]. Current information technology is based on classical physics, and we expect interesting perspectives if the laws of quantum physics are applied to this branch of science. The conceptual link between quantum mechanics and information processing was proposed by Feynman [3] and Deutsch [4] in the early 1980's. A decade later, an astonishing example of the power of quantum information processing was given by Shor in an algorithm for factorizing large numbers into primes [5]. Shor proved that the computational time can be polynomial with the input size for a quantum computer, while it grows exponentially in the case of conventional (classical) information processing. As a further motivation towards the interest in research on quantum information processing, let us refer to Moore's law, which states that about every one and half years the microprocessors of our personal computers double their speed while simultaneously reducing their size by a factor two. By the time of writing it is not clear to what extent the present silicon technology will stand to such a terrific pace. However, it seems foreseeable that in a not too distant future the logical gates of computers' microprocessors will be so small to consist of only a few atoms each. One then expects that the laws of quantum mechanics will significantly affect the processing of information.

This article is organized as follows. We first briefly recall the basic conditions for implementing a quantum algorithm, pointing out the present state of the art achieved in several branches of experimental physics. We here focus on the prospects of cold atoms trapped in mesoscopic optical lattices for scalable quantum computing. Subsequently, we review experimental work of our group concerning the resolving and addressing atoms in individual sites of a CO_2-laser optical lattice and forced evaporation of ultracold rubidium atoms in such optical microtraps. We finally discuss future prospects.

19.2 Entanglement and Beyond

The possibility to operate with coherent superpositions and entangled states is essential for a quantum computer [6]. There are several conditions that a set of real quantum objects must fulfill in order to allow for the application of quantum computing. First of all, we require a quantum register, as e.g. several two-level quantum systems which are isolated from the environment for sufficiently long to maintain coherence throughout the computation process. We then should envision a mechanism for coupling the two-level systems by performing unitary gate operations, in other words we have to implement a quantum bus channel connecting our quantum objects, the so called quantum bits (qubits). And last but not least, we have to employ a technique for reading-out the final result of our computation. This last requirement is not only needed to work out the outcomes of the whole process, but it is also necessary to set the quantum register to a well known initial state [7]. So far, an increasing number of theoretical proposals towards the physical implementation of quantum gates has been published. Cirac and Zoller [8] suggested to implement quantum logic in coherent superpositions of two hyperfine ground states of cold ions trapped in a Paul trap. Wineland and coworkers experimentally demonstrated a controlled-NOT gate with a single trapped ion [9]. This (and other) early experiments have successfully demonstrated the operational principle of quantum logical gates. In ion traps, the implementation of real quantum algorithms, which require many entangled particles, is ultimately limited by decoherence originated by the Johnson-noise of the trap endcaps. Other experimental techniques have been implemented for the realization of quantum logic gates: cold atoms in high-finesse cavities [10] and nuclear spins with NMR techniques [11]. In 'flying qubits' cavity-QED experiments the quantum register consists of photons of an optical cavity. These modes are coupled to others via an atom placed inside the cavity. In NMR experiments, the quantum register is formed by nuclear spins of molecules in a strong magnetic field, and the quantum bus channel is provided by spin-spin interactions. In both cases the scalability poses tough limitations to the construction of a quantum processing machine. For example, NMR techniques suffer from an exponential decrease of the signal–to–noise ratio after only few quantum gates. Several interesting proposals on quantum logic gates in solid state devices have been published. In principle, solid state devices are easy to scale up, but nonetheless their main drawback is still represented by decoherence caused by the strong interaction with a complex environment.

A recently proposed technique for implementing and testing quantum logical gates with neutral atoms uses far detuned optical lattices. In optical lattices, atoms are trapped in the nodes or antinodes of optical standing-waves [12]. Several researchers suggested that these systems are attractive and effective tools for quantum information processing [13–16]. In optical lattices, the quantum bits can be encoded in internal hyperfine state of atoms, with a single trapped atom per lattice site. The lattice can then be regarded as a very dense and periodic quantum register, in which it is possible to perform multiple-particle entanglement operations in parallel. The quantum bus channel can e.g. be implemented by using a state dependent lattice potential and controlled elastic collisions between atoms in adjacent lattice sites, as proposed by Jaksch *et al.* [15] (see also Ref. [14]). It has been pointed out that in such systems efficient schemes for quantum error corrections and fault-tolerant computing can be straightforwardly implemented due to the inherent possibility of parallel operation [15, 17]. The addressing of single qubits is facilitated when using a trapping wavelength far above that of the atomic absorption wavelength. Optical lattices based on the focused and retroreflected radiation derived from a CO_2-laser operating near 10.6 μm seem to be promising candidates for such experiments.

19.3 Quantum Logic and Far-detuned Optical Lattices

In optical lattices, atoms are trapped in light-shift potentials created by the interference of two or more laser beams. The nature of the trapping force arises from the coherent interaction between the induced atomic dipole moment and the laser electric field [18–20]. When the laser frequency is tuned to the red side of an atomic resonance, the dipole force attracts atoms towards the interference maxima of the light field. For optical fields with frequency far below all electric dipole resonances of ground state atoms (i.e. 'quasistatic' fields), the trapping potential is given by

$$U = -\frac{1}{2}\alpha_s|\vec{E}|^2 \tag{19.1}$$

where α_s denotes the static atomic polarizability of the ground state and $\vec{E}$ is the electric field associated with the optical field. Due to the large detuning, the photon scattering rate is very small. In particular, the Rayleigh photon scattering rate in the quasistatic regime is given by the following expression

$$\Gamma_S = \frac{16 r_0^2 P}{3\hbar w_0^2}(\frac{m_e \alpha_s}{e^2})\omega^3 \tag{19.2}$$

where w_0 is the laser beam waist, r_0 is the classical electron radius, m_e is the electron mass and ω denotes the optical frequency of the laser light. The ω^3 term is a phase space factor which, in addition to the large detuning from resonance, reduces the photon scattering for laser fields with small optical frequency. Spontaneous Raman scattering is suppressed by a further factor $(\Delta_{\mathrm{FS}}\omega/\omega_{\mathrm{atom}})^2$, where ω_{atom} is the frequency of the atomic resonance. In our experiments we use CO_2-laser light whose wavelength is near 10.6 μm, and typical values of the Rayleigh scattering rate on trapped rubidium atoms are of the order of 600 s. This results in a small coupling of the atoms to the environment, so that the effect of decoherence can be kept small.

The addressing of an individual qubit in the lattice by means of focused, resonant laser beams requires the optical resolving of the lattice sites. An optical resolving is possible when the spatial distance between adjacent lattice sites $\lambda_{\mathrm{laser}}/2$ is much larger than the wavelength of illumination, that is the atomic absorption wavelength λ_{atom}. This criterion is well fulfilled in our experiments, where the lattice spacing of 5.3 μm is almost an order of magnitude above the absorption wavelength of the rubidium D2 line (780 nm).

When a lattice potential that depends on the internal atomic state is used, local interactions (as elastic collisions) can produce an entanglement of atoms. We here focus on such local techniques, as they may ultimately lead to highly parallel quantum gates. The internal atomic structure plays an important role in the following discussion. For alkali atoms trapped in an extremely far-detuned laser field, the detuning from resonance is much larger than both

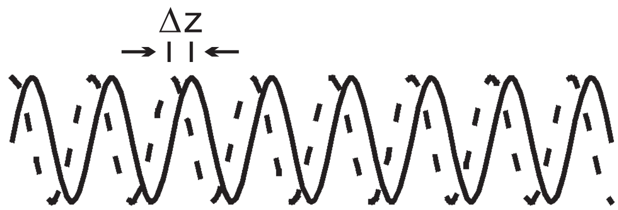

Figure 19.1: Spatial intensity dependence of two 1D standing-waves with σ^+ (solid), σ^- (dashed) respectively circular polarization. The two standing-waves are spatially shifted relatively to each other by Δz. For a suitable laser detuning, atoms in the ground-state level $|g+\rangle$ are pulled into the intensity maxima of the σ^+-polarized standing-wave, whereas atoms in the $|g-\rangle$ state are trapped in the maxima of the σ^--polarized standing-wave.

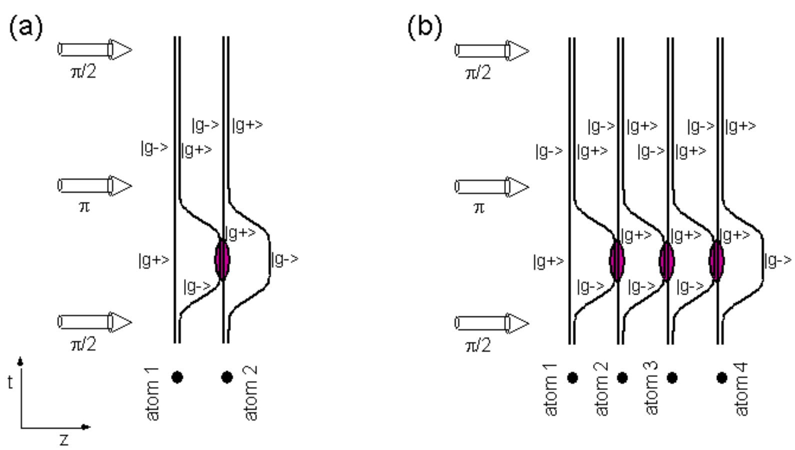

Figure 19.2: Scheme of a quantum logic gate for (a) two and (b) four atoms. The quantum bits are stored in each atom as a coherent superposition of the ground-state levels $|g+\rangle$ and $|g-\rangle$. In shaded regions, matter-waves are phase shifted by cold coherent collisions.

the hyperfine and fine structure splitting. This condition is met when CO_2-laser radiation is used. The trapping potential for ground-state alkali atoms here corresponds to that of a $J = 0$ to $J' = 1$ transition, as the ac Stark shift for all ground-state sublevels is identical and does not depend on the internal atomic state. However, a state-dependent lattice potential can be obtained when introducing additional laser beams with detuning comparable to the upper state fine structure splitting, but still large compared to the hyperfine structure. In this case, the electron spin can no longer be neglected and one can show that the ac Stark shift depends on the laser polarization. Thus, the idea is to transfer the atoms trapped in CO_2-laser field into a closer resonant manipulation lattice during gate operations. The manipulation lattice with laser detuning comparable to the atomic fine structure splitting, i.e. tuned between the $P_{1/2}$ and $P_{3/2}$ levels, produces an ac Stark shift depending on the polarization of the light field and, for a particular detuning, some of the ground state magnetic sublevels are trapped in σ^+ polarized light, while others in σ^- polarized light. It is then possible to distinguish two atomic "species" which can be manipulated individually with two oppositely circularly polarized standing waves. When the qubits are stored in a coherent superposition of two ground state sublevels $|g+\rangle$ and $|g-\rangle$, which are trapped in σ^+ and σ^- polarized light respectively, a quantum logic phase gate can be realized with a transient spatial shift operation of e.g. the $|g+\rangle$ components by one lattice separation, leading to a cold collision with the component in $|g-\rangle$ of the atom in the next lattice site, see Figs. 19.1 and 19.2. The interaction between two cold atomic wavepackets is determined by the s-wave scattering length and can be mathematically expressed in terms of a contact potential. The resulting interaction leads to a conditional phase shift in the atomic wavefunction [15]. Let us assume that a standing wave of the manipulation light is oriented along the same axis as the infrared wave generated by the CO_2-laser, and that the CO_2-laser wavelength is chosen such that it equals an integer multiple of the near-resonant light, e.g. $\lambda_{CO_2} = 13\lambda_{res}$. After preparing the qubits in the CO_2-laser lattice, the retroreflected 10.6 μm beam is extinguished and the closer resonant light is activated. The atoms are then transferred into the near-resonant standing-wave and they occupy precisely every 13th lattice site. In this near-resonant lattice conditional dynamic can be implemented. The described scheme should enable the realization of entangled two and more particle quantum states with the possibility of addressing individual qubits.

19.4 Resolving and Addressing cold atoms in single lattice sites

In this section we review the realization of a mesoscopic optical lattice, implemented with cold atoms trapped in a CO_2-laser standing-wave [21]. Fig. 19.3 shows a scheme of the experimental setup, as used by our group while located at the Max-Planck-Institut für Quantenoptik (MPQ) in Garching near Munich. A single mode CO_2-laser generated up to 50 W mid-infrared radiation near 10.6 μm. The light passed through an acusto-optic modulator (AOM) in order to provide optical isolation and allow for a control of the beam intensity. The transmitted beam entered a vacuum chamber and was focused by an adjustable ZnSe lens placed inside the vacuum chamber to a beam waist of typically 35 μm. By means of a further lens and an external retroreflecting mirror an intense standing wave was formed. Atoms of the isotope ^{85}Rb were collected and pre-cooled in a magneto-optical trap (MOT), which was loaded from the thermal gas emitted by heated rubidium dispensers. The cooling light, tuned a few linewidth to the red of the $5S_{1/2}, F = 3$ to $5P_{3/2}, F = 4$ cycling transition, was emitted by a free-running diode laser injection locked to a second, grating-stabilized diode. In order to repump rubidium atoms into the cooling transition, a grating-stabilized third laser locked to the $5S_{1/2}, F = 2$ to $5P_{3/2}, F = 3$ transition was used.

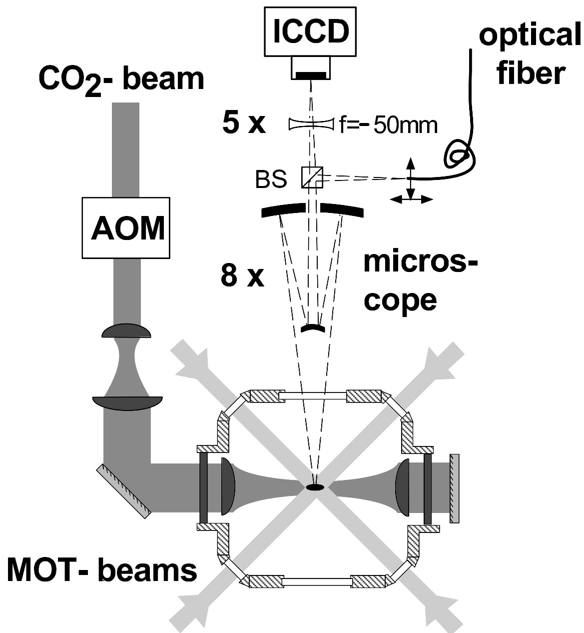

Figure 19.3: Schematic of the experimental apparatus.

During a typical experimental run, rougly 5×10^7 atoms were collected in the MOT during a 3s loading phase. Then they were compressed for 20 ms in a temporal dark MOT [22] realized by further detuning the cooling laser and by simultaneously reducing the repumping laser intensity by a factor 10. During this phase, the CO_2-laser beam was switched on, allowing for rubidium atoms to be loaded into its focal region. At the end of the dark MOT phase, all resonant beams were extinguished and the magnetic field was switched off. By this time, rubidium atoms were only trapped by the lattice potential. In order to detect the trapped atoms, the MOT beams were pulsed on after a variable amount of time, and the fluorescence scattered by the trapped atoms was imaged onto both a calibrated photodiode and an intensified CCD camera (ICCD). The typical numbers of atoms trapped in the lattice was near 1×10^6. These atoms were distributed over more than 100 pancake-shaped lattice sites. The trap lifetime was 3.4 s, being limited by collisions with the thermal background gas (10^{-9} mbar background pressure). With an mid-infrared input power of 14 W, the trap depth [13] was $U_0/\hbar = 43.5$ MHz, corresponding to a temperature of 1.4 mK. The vibrational frequencies of the CO_2 laser lattice were measured by parametrically exciting the trapped atoms [13]. For this measurement, we periodically modulate the CO_2-laser beam intensity with an AOM. We observed a significant trap loss, caused by parametric vibrational excitation, when the modulation frequency was close to twice a trap vibrational frequency. With typical parameters of 14W optical power and 35 μm waist radius it was possible to measure oscillation frequencies in the central trap region of $\nu_z = 54(5)$kHz in the axial and $\nu_r = 4.2(5)$kHz in the radial direction. For these parameters the Lamb-Dicke limit, corresponding to an oscillation frequency above the photon recoil energy in frequency units $\nu_{rec} = h/2m\lambda^2$(3.8 kHz for ^{85}Rb), is therefore fulfilled in all three spatial dimensions. For a more complete characterization of the trap, the atomic temperature was measured with a time–of–flight technique. The observed values were strongly depended on the trapping laser power. This power dependence is attributed to the difference in the ac Stark shifts of ground and excited states of the rubidium atoms, which for high laser powers becomes comparable to the upper-state hyperfine splitting, and then significantly reduces the efficiency of sub-Doppler cooling mechanisms. For maximum laser power, the measured temperatures approached the Doppler limit of the rubidium atom (140μK), while for small CO_2-laser power (near 4 W power in the trapping beam), we observed temperatures as low as 10μK. At those low values of the laser power we measured the maximum atomic phase space density $n\lambda_{dB}^3$ of about 1/300 in the optical lattice, see [23]. The tight confinement in the steep microtraps gave an atomic phase space density roughly three orders of magnitude above that of a conventional MOT. The atomic density reached values of several $10^{13}\ \mathrm{cm}^{-3}$, leading to a high collisional rate.

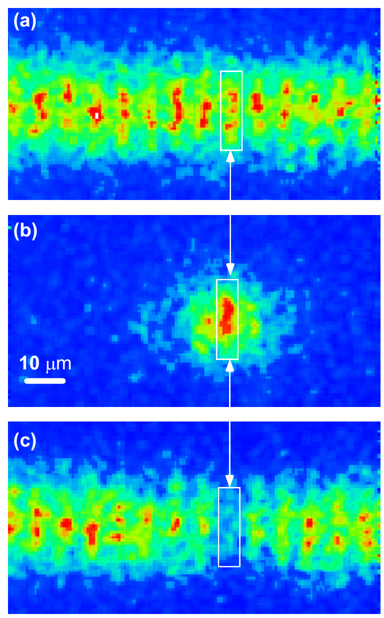

Figure 19.4: Images of the lattice after the following manipulations: (a) No manipulation of the atoms in the micro-traps. (b) Only atoms from a single lattice site are illuminated during the exposure with a focused laser beam. (c) Image of the lattice after removing atoms in one lattice site before the exposure.

Finally, it was possible to spatially resolve atoms trapped in single lattice sites, see Fig. 19.4. For this imaging of the lattice, the power of the CO_2-laser trapping field was lowered to 4 W, which reduces the atomic velocity distribution spread. The trapped atoms were irradiated with resonant light by pulsing on the MOT beams for a period of up to 100 μs. The frequency of this light was chosen to be resonant with the $5S_{1/2}, F = 3$ to $5P_{3/2}, F = 4$ transition at the bottom of the central potential wells. During the exposure, the MOT repumping light was also activated. The scattered atomic fluorescence was imaged by a long-distance microscope (1.9 μm spatial resolution) placed 10 cm away from the trap center outside the vacuum system onto an ICCD camera. Fig. 19.4a shows rubidium atoms localized in the periodically spaced pancake-like micro-traps of 5.3 μm period. Each of these sites contained up to 4×10^3 atoms. The CO_2-laser trapping beam was left on during the entire cycle. Fig. 19.4b depicts an image taken by only illuminating a single trapping site for a period of 100 μs. Here, around 10 μW of additional resonant light was sent through the core of an optical fiber and then imaged via a beamsplitter through the microscope onto the sample. Repumping light was again provided by the MOT rempumping beams. The exposure shows atoms localized in one distinct potential well of the standing wave, with the neighboring lattice sites suppressed by a factor of approximately 2.3. The other lattice sites were filled, but not visible here. Finally, for the image shown in Fig. 19.4c, a single lattice site was removed before the exposure with an intense resonant laser beam. Here, after loading the atoms into the trap, a 10 μs long pulse of light through the fiber with the same frequency, but with 20 times higher intensity, was applied. Again the MOT repumping beams were used to provide the necessary repumping light. The population of a single lattice site was almost completely removed, while atoms in the neighboring sites had been affected much less by the short pulse. By varying the position of the optical fiber along the axial direction of the lattice it was possible to address different lattice site within the optical field of view, which comprised around 50 lattice sites. These pictures demonstrate that it is in principle possible to address single qubits, as is necessary to read in and out quantum information in our optical lattice.

19.5 Recent work

To prevent decoherence during gate operations, it is mandatory to cool the atoms into the vibrational ground state of the lattice potential [15]. Such ground state cooling can be achieved either by using Raman sideband cooling technique [24] or by forced evaporation of trapped atoms [25, 26]. Given the high atomic densities several $10^{13}\,\mathrm{cm}^{-3}$ possible in CO_2-laser traps with laser cooling alone (discussed in the previous section) [23], the initial conditions seem especially good for evaporative cooling techniques. Recent other work has impressively shown that forced evaporation in CO_2-laser traps can achieve rapid cooling to quantum degeneracy [27, 28]. In our experiment, we have obtained initial results on evaporative cooling of ^{87}Rb atoms in a dipole trap formed by two intersecting CO_2-laser beams crossing at an angle of 45 degrees. The whole loading cycle of this trap was very similar to that of the far-detuned lattice discussed above. To achieve lower background pressure, the dispenser current was reduced. Within a loading time of 5 s we collected 1×10^7 atoms into the MOT. Subsequently, a 50 ms long dark MOT phase applied. Throughout this cycle the infrared CO_2-laser radiation was left on. After extinguishing the near-resonant cooling beams and the MOT magnetic field, the atoms were again trapped in the far-detuned field only. The transfer efficiency from the MOT to the crossed dipole trap here was near 10 percent, resulting in some 1×10^6 trapped atoms at an initial atomic temperature of 70 μK, for maximum CO_2-laser power of 15 W in each beam. By parametrically exciting the atoms, the trap vibrational frequencies were measured. Together with the measured atomic temperature and the total number of atoms this allowed us to infer the initial collisional rate to be about 5–6 kHz in the 45 degrees crossed dipole trap. The initial atomic phase space density of 1/200 (achieved by laser cooling only) was comparable to our previous result in the CO_2-laser optical lattice [23]. In order to achieve further cooling, the potential depth was lowered in a controlled way. This was achieved by reducing the trapping laser beam intensity via a reduction of the rf drive frequency power of the acousto-optic modulators. Evaporative cooling proceeded as atoms from the high energy tail of the thermal distribution of the trap were selectively allowed to escape, and subsequently the remaining atoms rethermalized towards a distribution with lower temperature. We tailored a combination of several linear intensity ramps to allow for a step by step optimization of the final phase space density. Fig. 19.5 shows time of flight fluorescence images of a typical evaporation run in the CO_2-crossed dipole trap. The final atomic temperature and density here are 1 μK and $10^{13}\,\mathrm{cm}^{-3}$ respectively, corresponding to an atomic phase space density of 1/15. To our belief, the final atomic phase spaced in these measurements is mostly limited by the crossing angle of the CO_2-laser beams, which for the vacuum chamber used in these measurements was limited to a maximum of 45 degree. For larger crossing angles, the atomic cloud be more strongly compressed, which is expected to increase both the collisional rate and phase space density. This assumption is supported by measurements of a crossed dipole trap with the even smaller crossing angle of 15 degrees, for which the phase space density during forced evaporation was observed to only increase by a factor three.

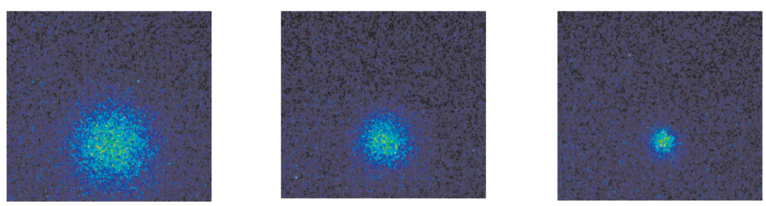

(a) (b) (c)

Figure 19.5: Images of the crossed dipole trap after 15 ms expansion. The phase space density (psd) has been calculated by measuring the trap vibrational frequencies, the atomic temperatures and the number of atoms remaining in the trap for different final potential depths. (a) Before forced evaporation; psd: 1/200. (b) During forced evaporation; psd: 1/60. (c) After evaporation; psd: 1/15.

In the last months of 2001, our group has moved from the MPQ to the Universität Tübingen. We took this move as an opportunity to implement some new concepts and redesigns of the experimental apparatus. To address the immediate experimental plans on evaporative cooling, our new vacuum chamber now allows for a 90 degrees crossing angle of the mid-infrared dipole trapping beams. The design of the new apparatus furthermore allows for a two-dimensional mesoscopic optical lattice while simultaneously giving an improved optical access, as is required for preparation and manipulation of lattice sites. We use a single frequency CO_2-laser with improved stability delivering an output power of 55 W. In the beginning of July 2002, we have observed first dipole trapping of atoms in the Tübingen lab. We are currently characterizing both simple and crossed dipole traps in detail, and are working towards the production of a 2D CO_2-laser lattice in which we plan to evaporatively cool the atoms to the ground state. This should yield a mesoscopic periodic array of Bose-Einstein microcondensates, in which the individual sites are individually addressable by means of focused laser beams. In this system, we expect novel possibilities in the direct microscopic study of quantum tunneling and quantum phase transitions. Unity occupation of lattice sites (as is required for quantum logic) can be achieved by making use of a phase transition from a superfluid Bose-Einstein phase to a Mott insulator phase induced when increasing the ratio between the on-site interaction potential to the tunnelling matrix element. Such a phase transition is predicted by the Bose-Hubbard model [29] and has recently been demonstrated experimentally in a near resonant optical lattice [30]. To conclude, optical lattices are of interest in a wide spectrum of physical fields ranging from model systems for solid state theory to its fascinating prospects in studies of entangled states and scalable quantum logic.

We acknowledge the contributions of F.S. Cataliotti, S. Friebel, T.W. Hänsch, and J. Walz during the Munich phase of this project, and we thank H. Briegel and P. Zoller for useful and stimulating discussions. Finally, we acknowledge support from the Deutsche Forschungsgemeinschaft and an EC science program cooperation.

References

[1] K. Mattle, H. Weinfurter, P. G. Kwait, and A. Zeilinger, Phys. Rev. Lett. **76**, 4656 (1996); A. Furusawa, J. L. Sørensen, S. L. Braunstein, C. A. Fuchs, H. J. Kimble, and E. S. Polzik, Science Oct 23, 706-709, (1998); D. Boschi, S. Branca, F. De Martini, L. Hardy, and S. Popescu, Phys. Rev. Lett. **80**, 1121 (1998).

[2] M. Inguscio, S. Stringari, C. Wieman, (Eds.), ”Bose-Einstein Condensation in Atomic Gases.”, Amsterdam: IOS Press, (1999).

[3] R. P. Feynman, “Simulating Physics with computers,” Int. J. Theor. Phys. **21**, p. 467, (1982).

[4] D. Deutsch, “Quantum theory, the Church-Turing principle and the universal quantum computer”, *Proc. Roy. Soc.* A **400**, 97, (1985).

[5] P. W. Shor, “Algorithms for quantum computation: Discrete logarithms and factoring”, *Proc. 35th IEEE Symposium on Fundations of Computer Science*, S. Goldwasser, Ed. Los Alamos, CA: IEEE Computer SOC. Press, (1994), p. 124.

[6] C. H. Bennett, “Quantum Information and Computing”, Physics Today, 24, October 1995.

[7] D. P. DiVincenzo, “The Physical Implementation of Quantum Computation”, quant-ph/0002077.

[8] J. I. Cirac, P. Zoller, Phys. Rev. Lett. **74**, 4091 (1995).

[9] C. Monroe, D. M. Meekhof, B. E. King, W. M. Itano, D. J. Wineland, Phys. Rev. Lett. **75**, 4714, (1995).

[10] Q. A. Turchette, C. J. Hood, W. Lange, H. Mabushi, H. J. Kimble, Phys. Rev. Lett. **75**, 4710, (1995).

[11] N. A. Gershenfeld and I. L. Chuang, “Bulk spin-resonance quantum computing”, *Science* **274**, 350 (1997).

[12] P. S. Jessen and I. H. Deutsch, Adv. At., Mol., Opt. Phys. **37**, 95 (1996), and references therein.

[13] S. Friebel, C. D'Andrea, J. Walz, M. Weitz, and T. W. Hänsch, Phys. Rev. A **57**, R20 (1998).

[14] G. Brennen, C. Caves, P. Jessen and I. Deutsch, Phys. Rev. Lett. **82**, 1060 (1999).

[15] D. Jaksch, H.-J. Briegel, J. I. Cirac, C. W. Gardiner, and P. Zoller, Phys. Rev. Lett. **82**, 1975 (1999).

[16] A. Hemmerich, Phys. Rev. A **60**, 943 (1999).

[17] H.-J. Briegel, T. Calarco, D. Jaksch, J. I. Cirac, and P. Zoller, Journal of Modern Optics **47** N. 2/3, 415 (2000).

[18] S. Chu, J. E. Bjorkholm, A. Ashkin, and A. Cable, Phys. Rev. Lett. **57**, 314 (1985); see also: R. Grimm, M. Weidemüller, Yu. B. Ovchinnikov, Adv. At. Mol. Opt. Phys. **42**, 95 (2000).

[19] C. Cohen-Tannoudji, "Atomic Motion In Laser Light", J. Dalibard, J. M. Raimond and J. Zinn-Justin, eds. Les Houches, Session LIII, 1990 Elsavier Science Publisher B.V., 1992.

[20] J. P. Gordon, A. Ashkin, "Motion of atoms in a radiation trap", Phys. Rev. A **21**, 1606 (1980).

[21] R. Scheunemann, F. S. Cataliotti, T. W. Hänsch, M. Weitz, Phys. Rev. A **62** 51801 **R**, (2000).

[22] W. Ketterle, K. B. Davis, M. A. Joffe, A. Martin, D. E. Pritchard, Phys. Rev. Lett. **70**, 2253 (1997).

[23] S. Friebel, R. Scheunemann, J. Walz, T. W. Hänsch and M. Weitz, Appl. Phys. B **67**, 699 (1998).

[24] S. Hamann, D. Haycock, G. Klose, D. Pax, I. Deutsch, and P. Jessen, Phys. Rev. Lett. **80**, 4149 (1998); H. Perrin, A. Kuhn, I. Bouchoule, and C. Salomon, Europhys. Lett. **42**, 395 (1998); V. Vuletic, C. Chin, A. Kerman, and S. Chu, Phys. Rev. Lett. **81**, 5768 (1999).

[25] K. B. Davis, M.-O. Mewes, W. Ketterle, Appl. Phys. B **60**, 155 (1995).

[26] C. S. Adam, H. Jin Lee, N. Davidson, M. Kasevich, and S. Chu, Phys. Rev. Lett. **74**, 3579, (1995).

[27] M. D. Bennett, J. A. Sauer, and M. S. Chapman, Phys. Rev. Lett. **87**, 10404 (2001).

[28] S. R. Granade, M. E. Gehm, K. M. O'Hara, and J. E. Thomas, Phys. Rev. Lett. **88**, 120405, (2002).

[29] D. Jaksch, C. Bruder, J. I. Cirac, C. W. Gardiner, and P. Zoller, Phys. Rev. Lett. **81**, 3108 (1998).

[30] M. Greiner, O. Mandel, T. Esslinger, T. W. Hänsch, and I. Bloch, Nature **415**, 39 (2002).